On the Correlation and Scattering Functions of the WSSUS Channel for Mobile Communications

John S. Sadowsky, *Member, IEEE,* and Venceslav Kafedziski, *Student Member, IEEE*

***Abstract*— The wide-sense stationary-uncorrelated scattering (WSSUS) channel model is a commonly employed model for the multipath channel experienced in mobile communications. The second-order statistics of these channels are described by the *delay cross-power density* $\phi_h(\tau;\Delta t)$ or by its Δt-Fourier transform, the *scattering function* $S_h(\tau;\lambda)$. This paper presents an analysis of the delay cross-power density and scattering functions for mobile communications channels. We assume an arbitrary spatially uncorrelated scattering (US) field with arbitrary propagation-loss factors. Our first result is a general integral expression for $\phi_h(\tau;\Delta t)$ that holds with both transmitter and receiver being mobile. We then derive more detailed results for the case of a stationary base station. We derive an infinite Bessel series for $\phi_h(\tau;\Delta t)$ and a closed-form expression for $S_h(\tau;\lambda)$. These results generalize the well-known classical approximation for the time-correlation function $\bar{\phi}_h(\Delta t) \stackrel{\text{def}}{=} \int \phi_h(\tau;\Delta t)\,d\tau \approx J_0(2\pi\lambda_m\Delta t)$, which corresponds to the zeroth term of our Bessel series.**

I. Introduction

Let $h(\tau;t)$ denote the time-varying complex baseband impulse response of a multipath channel. When a narrowband signal $x(t) = \mathrm{Re}\{\tilde{x}(t)e^{j2\pi f_c t}\}$ having complex envelope $\tilde{x}(t)$ and center frequency f_c is transmitted, the received narrowband signal $Y(t) = \mathrm{Re}\{\tilde{Y}(t)e^{j2\pi f_c t}\}$ has complex envelope

$$\tilde{Y}(t) = \int h(\tau;t)\tilde{x}(t-\tau)\,d\tau.$$

We consider multipath channels that are randomly varying in time. The channel is said to exhibit *delay uncorrelated scattering* (US) if

$$\frac{1}{2}\mathrm{E}[h(\tau_a;t_1)^* h(\tau_b;t_2)] = \phi_h(\tau_a;t_1,t_2)\,\delta(\tau_b-\tau_a) \quad (1)$$

and it is *wide-sense stationary* (WSS) if $\phi_h(\tau;t_1,t_2) = \phi_h(\tau;t_2-t_1)$. The second-order statistics of the wide-sense stationary-uncorrelated scattering (WSSUS) channel are represented by its *delay cross-power density* $\phi_h(\tau;\Delta t)$ or by the *scattering function*

$$S_h(\tau;\lambda) \stackrel{\text{def}}{=} \int \phi_h(\tau;\Delta t)e^{-j2\pi\lambda\Delta t}\,d\Delta t. \quad (2)$$

where $S_h(\tau;\lambda)$ is just the Δt-Fourier transform of $\phi_h(\tau;\Delta t)$ and λ is the Doppler frequency variable. Other related functions of interest include the *multipath intensity profile* $\phi_h(\tau) \stackrel{\text{def}}{=} \phi_h(\tau;0) = \int S_h(\tau;\lambda)\,d\lambda$, the *time-correlation function* $\bar{\phi}_h(\Delta t) \stackrel{\text{def}}{=} \int \phi_h(\tau;\Delta t)\,d\tau$, and the *Doppler power spectrum* $S_h(\lambda) = \int S_h(\tau;\lambda)\,d\tau$. [$\phi_h(\tau)$ is also known as the *delay power spectrum*]. See [3] or [15, ch. 14] for general expositions on these WSSUS channel statistics.

There has been a good deal of research into the particular WSSUS channels that arise in mobile communications [1], [2], [4]–[10], [12], [13], [16], [18]. The classical result was derived by Clarke [5], and later by Jakes [13], for the case of a mobile communicating with a stationary base in a two-dimensional (2-D) propagation geometry. [Aulin [1] derives three-dimensional (3-D) generalizations.] These well-known results state that

$$\bar{\phi}_h(\Delta t) \propto J_0(2\pi\lambda_m\Delta t) \quad \text{and} \quad S_h(\lambda) \propto \frac{1}{\sqrt{\lambda_m^2-\lambda^2}}$$

for $|\lambda| \le \lambda_m$, where $\lambda_m = \frac{v}{c}f_c$ is the maximal Doppler frequency for a mobile speed v, carrier frequency f_c, and speed of propagation c. The Clarke/Jakes derivations are based on the assumption that the physical scattering environment is so chaotic that at the mobile, the angle of arrival of a received plane wave is a uniformly distributed random variable. This assumption seems plausible for urban environments, but perhaps not in the suburban or rural environments. Suburban or rural scattering fields are much less dense, and potentially strong scatterers located far from the mobile result in much larger multipath delay spreads than would be typical for the urban case.

A consequence of the Clarke/Jakes assumption is that the results do not depend on the mobile's direction of travel. In addition, the time-correlation function is strictly real valued, and the Doppler power spectrum is symmetric. Conversely, a *non*uniform distribution of the angle of arrival will skew the Doppler power spectrum, which corresponds to a nonzero imaginary component of the correlation function. For example, if the angle of arrival is biased in the direction of the base station, then the Doppler power spectrum will be skewed toward $+\lambda_m$ when the mobile is moving toward the base and skewed toward $-\lambda_m$ when moving away the base.

Another consequence of the Clarke/Jakes assumption is *delay/temporal separability*, that is, $\phi_h(\tau;\Delta t) \propto \phi_h(\tau)\bar{\phi}_h(\Delta t)$, or equivalently, $S_h(\tau;\lambda) \propto \phi_h(\tau)S_h(\lambda)$. Often the Clarke/Jakes Doppler power spectrum is used with an ad hoc or perhaps measured multipath intensity profile $\phi_h(\tau)$. For example, an exponential intensity profile is a popular model for urban environments [12]. Separability is also commonly assumed in RAKE receiver analysis [15].

Manuscript received September 5, 1995; revised June 27, 1996.

The authors are with the Telecommunications Research Center, Department of Electrical Engineering, Arizona State University, Tempe, AZ 85287-7206 USA (e-mail: sadowsky@asu.edu).

Publisher Item Identifier S 0018-9545(98)00099-1.

In this paper, we present a new analysis that does not rely on the Clarke/Jakes uniform angle of arrival assumption. Consequently, our results do indicate dependency on the direction of travel angle θ_0 (relative to the base-mobile baseline), and $\phi_h(\tau;\Delta t)$ and $S_h(\tau;\lambda)$ are generally *not* separable. A main result derived here is the Bessel function series

$$\phi_h(\tau;\Delta t) \propto \psi_0(\tau)J_0(2\pi\lambda_m\Delta t) + 2\sum_{n=1}^{\infty} j^n\psi_n(\tau)\cos(n\theta_0)J_n(2\pi\lambda_m\Delta t).$$

The series coefficient functions $\psi_n(\tau)$ are determined by the physical model that includes the spatial scattering field distribution and the mean-square propagation losses (including shadowing). We will also derive a general closed-form expression for the scattering function $S_h(\tau;\lambda)$. Observe that Clarke's result is just the zeroth term in the above series. Moreover, since $J_n(0)=0$ for $n\neq 0$, we see that the multipath intensity profile $\phi_h(\tau)=\phi_h(\tau;0)$ is $\propto \psi_0(\tau)$.

Our main results are not delay/temporal separable. However, since $\int_{-\pi}^{\pi}\cos(n\theta_0)\,d\theta_0 = 0$ for all $n>0$, clearly

$$\int_{-\pi}^{\pi}\phi_h(\tau;\Delta t)\,d\theta_0 \propto \psi_0(\tau)J_0(2\pi\lambda_m\Delta t).$$

Thus, while mobile moving in a fixed (and known) direction results in a *nonseparable* WSSUS channel model, we do obtain separability when direction of travel is averaged out.

We present three numerical examples. In all three cases we consider a uniformly distributed scattering field. In the first case, the mean-square propagation losses are $\propto 1/r^2$. This might be a reasonable model for rural or suburban channels. Urban channels, on the other hand, must include strong shadowing, which in turn concentrates strong multipath scattering near the mobile. We present two examples with a mean-squared propagation-loss $e^{-r/\bar{r}}$ factor that represents the shadowing effect. For example, $\bar{r}=500$ m results in delay spreads in the 1–2 μs range, which is the typical for urban environments. The two urban model examples are $\bar{r}=r_0$ and $\bar{r}=0.2r_0$, where r_0 is the distance between the mobile and base. In the former case, the mobile is near the base station, while the latter might be a typical situation near a cell boundary.

We believe that our spatial analysis removing the Clarke/Jakes uniform angle of arrival assumption is an informative and perhaps significant contribution. However, we must point out that we still do make two important assumptions. First, we assume a *spatially uncorrelated* scattering field, which in turn yields a WSSUS channel. In reality, scattering elements are buildings and other large structures such as trees, hills, etc. As pointed out by Braun and Dersch [4], a receiver of bandwidth B has a *spatial resolution* of roughly c/B. If dimensions of physical scatterers are smaller than this spatial resolution, then the scatterers are indistinguishable from "point scatterers," and the spatially US approximation is plausible. For example, $B=200$ kHz (= the bandwidth of a GSM channel) and the spatial resolution is $c/B=1.5$ km. For $B=1.23$ MHz (= the bandwidth of a IS-95 CDMA channel), $c/B=250$ m. See Lauritzen *et al.* [14] for channel models that do not assume US.

Our second assumption is that we consider only single scatterer propagation paths. This assumption may be questionable in indoor propagation environments and perhaps in very cluttered urban environments, but it is a reasonable assumption for suburban and rural multipath models [4], [8].

II. The Spatial Scattering Field

In this section, we derive spatial response formulas for the received complex envelope $\tilde{Y}(t)$ resulting from the transmission of a signal $\tilde{x}(t)$. Both transmitter and receiver may be in motion, and the geometry may be 2-D or 3-D. Section A describes the propagation model. Section B derives an exact spatial response expression. Section C examines the appropriate narrowband and constant velocity approximations. The compound Poisson scattering field, which encompasses the model building framework of [4] and [8], is examined in Section D. Section E characterizes $\tilde{Y}(t)$ as a "proper complex process" and derives a spatial integral expression for its complex autocorrelation function.

A. The Scattering and Propagation Models

Let $\mathbf{r}$ denote the spatial coordinate vector. Let $\mathbf{r}_T(t)$ and $\mathbf{r}_R(t)$ denote, respectively, the transmitter and receiver positions, with respective velocity vectors $\mathbf{v}_T(t)=\dot{\mathbf{r}}_T(t)$ and $\mathbf{v}_R(t)=\dot{\mathbf{r}}_R(t)$. The transmitted narrowband signal is of the form $x(t)=\mathrm{Re}\{\tilde{x}(t)e^{j2\pi f_c t}\}$, where f_c is the carrier frequency and $\tilde{x}(t)$ is the complex envelope having bandwidth $W \ll f_c$. The carrier wavelength is $\ell_c \stackrel{\text{def}}{=} c/f_c$.

$Z(\mathbf{r};t)$ will denote the *spatial scattering field*. We assume a spatially uncorrelated and WSS scattering field. That is, the complex autocovariance is

$$\frac{1}{2}\mathrm{cov}[Z(\mathbf{r};t_1)^*, Z(\mathbf{r}';t_2)] = \phi_S(\mathbf{r};t_2-t_1)\delta(\mathbf{r}-\mathbf{r}') \quad (3)$$

and the "pseudo-autocovariance" is

$$\frac{1}{2}\mathrm{cov}[Z(\mathbf{r};t_1), Z(\mathbf{r}';t_2)] = \hat{\phi}_S(\mathbf{r};t_2-t_1)\delta(\mathbf{r}-\mathbf{r}') \quad (4)$$

and the mean field $\mu_S(\mathbf{r}) \stackrel{\text{def}}{=} \mathrm{E}[Z(\mathbf{r};t)]$. Ultimately, $\hat{\phi}_S(\mathbf{r};\Delta t)$ and $\mu_S(\mathbf{r})$ play no role in the final results, but condition (4) is still an important part of the US condition. The function $\phi_S(\mathbf{r};\Delta t)$ is the *spatial scattering intensity function*. Examples of stochastic fields of this type include Gaussian white noise fields, compound Poisson white noise fields (see Section D), and mixtures of these two.

$L_1(\mathbf{r};t)$ and $L_2(\mathbf{r};t)$ will denote, respectively, the loss factors for propagation paths $\mathbf{r}_T(t) \to \mathbf{r}$ (transmitter-to-scatterer) and $\mathbf{r} \to \mathbf{r}_R(t)$ (scatterer-to-receiver). These loss factors account for amplitude attenuation due to both propagation loss and directional antenna gain patterns. They may be complex quantities due, perhaps, to directional phase response of the antennas, but usually these are nonnegative real-valued quantities. Free-space propagation loss with an omnidirectional antenna is characterized as $|L_i(\mathbf{r};t)|^2 \propto \|\mathbf{r}_i(t)\|^{-2}$, where $\mathbf{r}_1(t)=\mathbf{r}-\mathbf{r}_T(t)$ and $\mathbf{r}_2(t)=\mathbf{r}-\mathbf{r}_R(t)$. It has been suggested [4], [8] that $|L_i(\mathbf{r};t)|^2 \propto \|\mathbf{r}_i(t)\|^{-\gamma}$ with $\gamma > 2$ is a more appropriate model for urban radio propagation. These loss factors may be random variables. Shadowing, for example, can be modeled as a lognormal random loss, with mean-square loss $\mathrm{E}[|L_i(\mathbf{r};t)|^2] \propto e^{-r/\bar{r}}$ for some $\bar{r} > 0$.

B. An Exact Spatial Response Formula

Consider a narrowband signal $x(t) = \mathrm{Re}\{\tilde{x}(t)e^{j2\pi f_c t}\}$ transmitted over the propagation path $\mathbf{r}_T \rightarrow \mathbf{r} \rightarrow \mathbf{r}_R$. The signal received at position $\mathbf{r}_R(t)$ at time t was transmitted from position $\mathbf{r}_T(t-\tau(\mathbf{r};t))$ at time $t-\tau(\mathbf{r};t)$, and the propagation delay $\tau(\mathbf{r};t)$ satisfies the nonlinear equation

$$c\tau(\mathbf{r};t) = \|\mathbf{r}_R(t) - \mathbf{r}\| + \|\mathbf{r} - \mathbf{r}_T(t - \tau(\mathbf{r};t))\|. \tag{5}$$

The time-delayed bandpass signal is

$$\begin{aligned} x(t-\tau) &= \mathrm{Re}\{\tilde{x}(t-\tau)e^{j2\pi f_c (t-\tau)}\} \\ &= \mathrm{Re}\{[\tilde{x}(t-\tau)e^{-j2\pi f_c \tau}]e^{j2\pi f_c t}\} \end{aligned}$$

which has complex envelope $\tilde{x}(t-\tau)e^{-j2\pi f_c \tau}$. The total complex gain for a propagation path $\mathbf{r}_T \rightarrow \mathbf{r} \rightarrow \mathbf{r}_R$ is $L_1(\mathbf{r};t-\tau(\mathbf{r};t))L_2(\mathbf{r};t)Z(\mathbf{r};t)\,d\mathbf{r}$. Thus, integrating over the entire spatial scattering field, we find that the total channel response is

$$\tilde{Y}(t) = \int \tilde{x}(t-\tau(\mathbf{r};t))L(\mathbf{r};t)Z(\mathbf{r};t)e^{-j2\pi f_c \tau(\mathbf{r};t)}\,d\mathbf{r} \tag{6}$$

where we have lumped the loss factors together as $L(\mathbf{r};t) \stackrel{\text{def}}{=} L_1(\mathbf{r};t-\tau(\mathbf{r};t))L_2(\mathbf{r};t)$.

C. Approximations

The spatial response formula (6) is simplified by applying approximations resulting from mobile speeds $\|\mathbf{v}_T\|$ and $\|\mathbf{v}_R\|$ that are very small in comparison to the speed of propagation c and by utilizing the narrowband condition $W \ll f_c$. The *maximal Doppler* frequency shift of the channel is $\lambda_m = (\|\mathbf{v}_T\| + \|\mathbf{v}_R\|)f_c/c$. Note that $\|\mathbf{v}\| \ll c$ implies $\lambda_m \ll f_c$. Another important parameter is the *coherence time* $(\Delta t)_c$; $\phi_h(\tau;\Delta t) \approx 0$ for $|\Delta t| > (\Delta t)_c$. By the Fourier transform relationship between $\phi_h(\tau;\Delta t)$ and $S(\tau;\lambda)$, we deduce that $(\Delta t)_c \approx 1/\lambda_m$, at least to the order of magnitude. Clearly, we need to characterize the correlation function only for $|\Delta t| < (\Delta t)_c$.

For radio communications, it is also appropriate to assume that the mobile velocity is constant on the time scale of $(\Delta t)_c$. For example, $f_c = 900$ MHz with a maximal mobile speed of 200 km/h yields a maximal Doppler (for two mobiles) $\lambda_m = 333$ Hz, and, hence, $(\Delta t)_c$ is on the order of 3 ms. This time scale is extremely fast relative to vehicular dynamics. Thus, we hereafter use $\mathbf{r}_T(t) = \mathbf{r}_T + \mathbf{v}_T(t-t_1)$ and $\mathbf{r}_R(t) = \mathbf{r}_R + \mathbf{v}_R(t-t_1)$, where $\mathbf{r}_T \stackrel{\text{def}}{=} \mathbf{r}_T(t_1)$, $\mathbf{r}_R \stackrel{\text{def}}{=} \mathbf{r}_R(t_1)$, and t_1 is some arbitrarily fixed reference time.

In order to simplify the notation a bit, we hereafter orient the coordinate system so that $\mathbf{r}_T = \mathbf{0}$. The baseline distance between transmitter and receiver will be denoted $r_0 \stackrel{\text{def}}{=} \|\mathbf{r}_R\|$. For a scatterer located at position $\mathbf{r}$, $r_1(\mathbf{r}) \stackrel{\text{def}}{=} \|\mathbf{r}\|$ is the

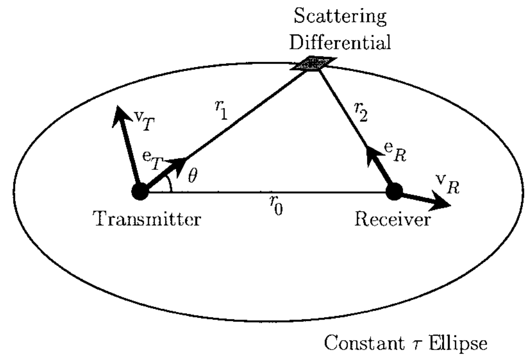

Fig. 1. Transmitter-scatterer-receiver geometry.

transmitter-to-scatterer distance and $r_2(\mathbf{r}) \stackrel{\text{def}}{=} \|\mathbf{r} - \mathbf{r}_R\|$ is the scatterer-to-receiver distance at time $t = t_1$. This geometry is illustrated in Fig. 1.

The first step is to derive a good linear approximation for $\tau(\mathbf{r};t)$ from (5) that accounts for time variations on the order $(\Delta t)_c$. The linearization about a fixed time t_1 is

$$\tau(\mathbf{r};t) \approx \tau(\mathbf{r};t_1) + \frac{\partial}{\partial t}\tau(\mathbf{r};t)\bigg|_{t=t_1}(t-t_1).$$

Since $\|\mathbf{v}_T\| \ll c$, the term $\|\mathbf{r} - \mathbf{r}_T(t_1 - \tau(\mathbf{r};t_1))\| \approx \|\mathbf{r} - \mathbf{r}_T(t_1)\| = r_1(\mathbf{r})$. Thus

$$\tau(\mathbf{r};t_1) \approx \tau(\mathbf{r}) \stackrel{\text{def}}{=} \frac{r_1(\mathbf{r}) + r_2(\mathbf{r})}{c}. \tag{7}$$

Next, differentiation of (5) leads to

$$\frac{\partial}{\partial t}\tau(\mathbf{r};t)\bigg|_{t=t_1} = -\frac{\frac{1}{c}(\mathbf{e}_T \cdot \mathbf{v}_T + \mathbf{e}_R \cdot \mathbf{v}_R)}{1 - \frac{1}{c}\mathbf{e}_T \cdot \mathbf{v}_T}$$

where $\mathbf{e}_T \stackrel{\text{def}}{=} (\mathbf{r} - \mathbf{r}_T(t))/r_1(\mathbf{r})$ and $\mathbf{e}_R \stackrel{\text{def}}{=} (\mathbf{r} - \mathbf{r}_R(t))/r_2(\mathbf{r})$ are the transmitter and receiver line-of-sight unit vectors to the scatterer. Since $\|\mathbf{v}_T\| \ll c$, the term $\mathbf{e}_T \cdot \mathbf{v}_T/c$ may be neglected in the denominator of the last display. Define the *Doppler frequency* variable

$$\lambda(\mathbf{r}) \stackrel{\text{def}}{=} \frac{f_c}{c}\{\mathbf{e}_T \cdot \mathbf{v}_T + \mathbf{e}_R \cdot \mathbf{v}_R\}. \tag{8}$$

Then $\frac{\partial}{\partial t}\tau(\mathbf{r};t)|_{t=t_1} \approx -\lambda(\mathbf{r})/f_c$, and the linear approximation of $\tau(\mathbf{r};t)$ becomes

$$\tau(\mathbf{r};t) \approx \tau(\mathbf{r}) - \frac{\lambda(\mathbf{r})}{f_c}(t-t_1). \tag{9}$$

Now, consider application of the approximation (9) to the channel response formula (6). By (9), putting $t_2 = t_1 \pm (\Delta t)_c$, we obtain the following bound for the maximal delay change:

$$|\tau(\mathbf{r};t_2) - \tau(\mathbf{r})| \le \left|\frac{\lambda(\mathbf{r})}{f_c}\right|(\Delta t)_c \le \frac{\lambda_m}{f_c}(\Delta t)_c = \frac{\lambda_m \ell_c}{c}(\Delta t)_c. \tag{10}$$

Since $(\Delta t)_c \approx 1/\lambda_m$, for this time scale $|\tau(\mathbf{r};t) - \tau(\mathbf{r})|$ is on the order of $1/f_c$. Since $\tilde{x}(t)$ is a low-pass signal with bandwidth $W \ll f_c$, we have the narrowband approximation $\tilde{x}(t - \tau(\mathbf{r};t)) \approx \tilde{x}(t - \tau(\mathbf{r}))$ for $|\Delta t| \le (\Delta t)_c$. The other place that $\tau(\mathbf{r};t)$ occurs in (6) is in the complex exponential.

Here, we do have to retain the Doppler term in (9) because we must account for the resulting temporal phase change. Thus, applying the above approximations to (6) yields

$$\tilde{Y}(t) = \int \tilde{x}(t - \tau(\mathbf{r}))L(\mathbf{r};t)Z(\mathbf{r};t) \times e^{-j2\pi[f_c\tau(\mathbf{r}) - \lambda(\mathbf{r})(t-t_1)]}\, d\mathbf{r}. \tag{11}$$

D. The Compound Poisson Scattering Field

At this point it is worthwhile to relate the above formulation to some practical model building issues. We do this in the context of the compound Poisson scattering field.

A compound Poisson scattering field is determined by scatterer positions $\mathbf{r}_1, \mathbf{r}_2, \cdots$, and for each position we have a complex valued *scatterer response process* $Z_k(t)$. The points $\mathbf{r}_k$ are samples from a spatial Poisson point process with *intensity function* $\nu(\mathbf{r})$. (For a region of space R, $N(R) =$ the number of $\mathbf{r}_k$s in R is a Poisson random variable with parameter $\nu(R) = \int_R \nu(\mathbf{r})\, d\mathbf{r}$, and for disjoint regions $R_1, \cdots, R_n$, the random variables $N(R_1), \cdots, N(R_n)$ are independent.) Given the scatterer positions $\mathbf{r}_1, \mathbf{r}_2, \cdots$, for each position $\mathbf{r}_k$ we have an associated response $Z_k(t)$. The $Z_k(t)$s are statistically independent and WSS. Each $Z_k(t)$ depends on the point process only through the position $\mathbf{r}_k$. The resulting scattering field is

$$Z(\mathbf{r};t) = \sum_k Z_k(t)\delta(\mathbf{r} - \mathbf{r}_k). \tag{12}$$

The field (12) applied to (11) results in the impulse response formula

$$h(\tau;t) = \sum_k L(\mathbf{r}_k;t)Z_k(t)e^{-j2\pi[f_c\tau(\mathbf{r}_k) - \lambda(\mathbf{r}_k)(t-t_1)]} \times \delta(\tau - \tau(\mathbf{r}_k)). \tag{13}$$

This last expression is useful for Monte Carlo channel simulation [8].

The second-order statistics of the $Z_k(t)$s are determined by a mean function $\mu_Z(\mathbf{r}) = \mathrm{E}[Z_k(t)]$ (which does not depend on t by the WSS assumption), the autocorrelation function

$$\phi_Z(\mathbf{r};\Delta t) = \frac{1}{2}\mathrm{E}[Z_k(t)^* Z_k(t + \Delta t)]$$

and the pseudo-autocorrelation

$$\hat{\phi}_Z(\mathbf{r};\Delta t) = \frac{1}{2}\mathrm{E}[Z_k(t) Z_k(t + \Delta t)].$$

Following the derivation in [11, p. 401], it is a straightforward task to show that the scattering field second-order statistics are $\mu_S(\mathbf{r}) = \nu(\mathbf{r})\mu_Z(\mathbf{r})$

$$\phi_S(\mathbf{r};\Delta t) = \nu(\mathbf{r})\phi_Z(\mathbf{r};\Delta t)$$

and

$$\hat{\phi}_S(\mathbf{r};\Delta t) = \nu(\mathbf{r})\hat{\phi}_Z(\mathbf{r};\Delta t).$$

Note that while $\phi_S(\mathbf{r};\Delta t)$ and $\hat{\phi}_S(\mathbf{r};\Delta t)$ are covariance functions, as defined in (3) and (4), they are determined by the autocorrelation (not covariance) functions $\phi_Z(\mathbf{r};\Delta t)$ and $\hat{\phi}_Z(\mathbf{r};\Delta t)$.

In the urban environment, discrete scatterers are buildings and other structures, not delta functions. However, as indicated in the introduction, if the scatterer dimensions are small in comparison to the spatial resolution $c/2W$, then position variations $\mathbf{r}_k + \boldsymbol{\delta}$ over the scatterer's surface produce delay variations that are smaller than the receiver's delay resolution $1/W$. Such scatterers are thus indistinguishable from spatial δ functions, and hence, the field model (12) is appropriate.

Following Braun and Dersch [4], a physical scatterer, say, a building, may be modeled as a collection of component scatterers. In this case, $\mathbf{r}_k$ would be interpreted as the centroid of a cluster of component scatterers. Let $\mathbf{r}_k + \boldsymbol{\delta}_{k,i}$ denote the ith component scatterer's position, and let $\Delta\tau_{k,i} \stackrel{\text{def}}{=} \tau(\mathbf{r}_k + \boldsymbol{\delta}_{k,i}) - \tau(\mathbf{r}_k)$ and $\Delta\lambda_{k,i} \stackrel{\text{def}}{=} \lambda(\mathbf{r}_k + \boldsymbol{\delta}_{k,i}) - \lambda(\mathbf{r}_k)$ denote the scatterer's differential delay and Doppler relative to the centroid delay $\tau(\mathbf{r}_k)$ and Doppler $\lambda(\mathbf{r}_k)$. If the component displacements are small in comparison to the spatial resolution ($\|\boldsymbol{\delta}_{k,i}\| < c/2W$), then we may make use of the narrowband approximation $\tilde{x}(t - (\tau(\mathbf{r}_k) + \Delta\tau_{k,i})) \approx \tilde{x}(t - \tau(\mathbf{r}_k))$. That is, a compound scatterer is still indistinguishable from a point scatterer. However, the small variations in Doppler will result in a fading of the compound scatterer's response. Let $A_{k,i}$ denote the amplitude of the ith component response. The phase of $A_{k,i}$ will include the factor $e^{-j2\pi f_c \Delta\tau_{k,i}}$. Component scatterer dimensions and displacements may be small relative to the spatial resolution, but generally will be large in comparison to the wavelength ℓ_c. Thus, the differential delay induced phase factor can result in a nearly uniform phase distribution for some of the $A_{k,i}$s. Combining the responses of all components and utilizing the narrowband approximation yields the total response

$$\sum_i A_{k,i} e^{-j2\pi[f_c\tau(\mathbf{r}_k) - [\lambda(\mathbf{r}_k) + \Delta\lambda_{k,i}](t-t_1)]} = Z_k(t)e^{-j2\pi[f_c\tau(\mathbf{r}_k) - \lambda(\mathbf{r}_k)(t-t_1)]}$$

where the total scatterer response process is

$$Z_k(t) = A_{k,0} + \sum_{i>0} A_{k,i} e^{j2\pi\Delta\lambda_{k,i}(t-t_1)}.$$

The $i = 0$ term is reserved for the large smooth reflecting surface component called the specular component [8]. For this component, $\boldsymbol{\delta}_{k,0} = 0$, $\Delta\tau_{k,0} = 0$, and $\Delta\lambda_{k,0} = 0$, which implies that the phase distribution of $A_{k,0}$ should allow little or no phase variation. Notice that this in turn implies that $\mu_Z(\mathbf{r}) \not\equiv 0$ and $\hat{\phi}_Z(\mathbf{r};t) \not\equiv 0$. Other components, $i > 0$, form the diffuse component, which is often modeled as a slow Rayleigh fading process [8].

We have considered a spatially distributed compound scatterer having small physical dimensions in comparison to the spatial resolution of the receiver. Due to the effect of slight differences in Doppler shifts relative to the centroid Doppler $\lambda(\mathbf{r}_k)$, such a scatterer may be approximated as a time-varying (fading) point scatterer. For the specific case that $Z_k(t) \equiv Z_k$ does not vary with time, we will say that the scattering field is *time invariant*. (Of course, a time-invariant scattering field does not imply that $h(\tau;t)$ is time invariant as we still have vehicular motion to account for.)

E. The Complex Process $\tilde{Y}(t)$

The received signal process $\tilde{Y}(t)$ has *proper complex symmetry* if the mean and pseudo-autocorrelation functions vanish, that is, $\mathrm{E}[\tilde{Y}(t)] \equiv 0$ and $\mathrm{E}[\tilde{Y}(t_1)\tilde{Y}(t_2)] \equiv 0$. In this case, the second-order moments of the process are completely determined by the *complex autocorrelation function* $R_{\tilde{Y}}(t_1, t_2) \stackrel{\text{def}}{=} \frac{1}{2}\mathrm{E}[\tilde{Y}(t_1)^*\tilde{Y}(t_2)]$.

In Appendix B, we give arguments to show that $\tilde{Y}(t)$ does generally have proper complex symmetry. In addition to the $W \ll f_c$ and $v \ll c$ approximations, our arguments are based on the following statistical conditions.

1) For any propagation path $\mathbf{r}_T \rightarrow \mathbf{r} \rightarrow \mathbf{r}_R$, $L_1(\mathbf{r}; t)$, $L_2(\mathbf{r}; t)$, and $Z(\mathbf{r}; t)$ are statistically independent.
2) For fixed θ, the moments of $L(\tau, \theta; t) = L_1(\mathbf{r}; t)L_2(\mathbf{r}; t)$ are essentially constant functions of t over time frames on the order of $(\Delta t)_c$ and are slowly varying functions of τ.
3) The scattering field statistics $\phi_S(\tau, \theta; \Delta t)$, $\hat{\phi}_S(\tau, \theta; \Delta t)$, and $\mu_S(\tau, \theta)$ are slowly varying functions of τ.

The result obtained in Appendix B is that $\tilde{Y}(t)$ does have proper complex symmetry if we neglect the direct path and scatterers very near the direct path. Specifically, $h(\tau; t) \neq 0$ only when $\tau - \tau_0 \gg 1/2f_c$, where $\tau_0 = r_0/c$ is the minimal delay. This should not be surprising since the direct path clearly will not have the random phase required for proper complex symmetry. But then, the direct path component should not be included in the multipath statistics as represented here by $\phi_h(\tau; \Delta t)$ and $S_h(\tau; \lambda)$.

The proper complex symmetry result is important. Without it, $\phi_h(\tau; \Delta t)$ is not a complete descriptor of the channel's second-order moments. Braun and Dersch [4] previously gave an argument resulting in proper complex symmetry for the Poisson scattering field discussed in the previous section. However, they assume that the scatterer response processes $Z_k(t)$ have a uniformly distributed random phase. In effect, their result obtains the proper complex symmetry for the channel $h(\tau; t)$ as a consequence of assumed proper complex symmetry of the scattering field $Z(\mathbf{r}; t)$. Here, we have shown that $\tilde{Y}(t)$ has proper complex symmetry even when $Z(\mathbf{r}; t)$ does not! Our extension is of some interest because the uniform phase assumption may not be physically justifiable for scattering fields with strong specular components.

Given proper complex symmetry, the second-order moments of $\tilde{Y}(t)$ are completely determined by the complex autocorrelation function $R_{\tilde{Y}}(t_1, t_2)$. In Appendix B, we determine that this autocorrelation function is

$$R_{\tilde{Y}}(t_1, t_2) = \int_{\tau_0}^{\infty} \tilde{x}(t_1 - \tau)^* \tilde{x}(t_2 - \tau) \times \int_{-\pi}^{\pi} \mathcal{L}_1(\tau, \theta)\mathcal{L}_2(\tau, \theta)\phi_S(\tau, \theta; \Delta t) \times J(\tau, \theta)e^{j2\pi\lambda(\mathbf{r})\Delta t}\, d\theta\, d\tau \tag{14}$$

where $\mathcal{L}_i(\mathbf{r}) = \mathrm{E}[|L_i(\mathbf{r}; t)|^2]$ is the *mean square propagation-loss* factor for the propagation path $\mathbf{r}_T \rightarrow \mathbf{r}$ when $i = 1$ and for the propagation path $\mathbf{r} \rightarrow \mathbf{r}_R$ when $i = 2$.

III. The Two-Dimensional Mobile Multipath Channel

In this section, we obtain expressions for $\phi_h(\tau; \Delta t)$ and $S_h(\tau; \lambda)$ for 2-D propagation geometry. The first section derives a general integral expression for $\phi_h(\tau; \Delta t)$. This first integral formula allows both transmitter and receiver to be mobiles. The rest of the section considers communications with a stationary base. Section B derives our Bessel function series for the correlation function, and Section C derives the corresponding scattering function series. Section C also derives a closed-form expression for time-invariant scattering fields. Section D gives the separability results discussed in the introduction.

The analysis of this section is carried out for the case of a transmitter at position $\mathbf{r}_T = \mathbf{0}$ and a receiver at position $\mathbf{r}_R = [r_0\ \ 0]^t$, as illustrated in Fig. 1.

A. A General Integral Expression for the Delay Cross-Power Density

Consider two fictitious channels each having the same impulse response $h(\tau; t)$. Signals $\tilde{x}_a(t)$ and $\tilde{x}_b(t)$ are transmitted over the two channels, and the respective responses are $\tilde{Y}_a(t) = \int h(\tau; t)\tilde{x}_a(t - \tau)\, d\tau$ and $\tilde{Y}_b(t) = \int h(\tau; t)\tilde{x}_b(t - \tau)\, d\tau$. Then, from (1) we find that the cross correlation between $\tilde{Y}_a(t)$ and $\tilde{Y}_b(t)$ is

$$R_{\tilde{Y}_a\tilde{Y}_b}(t_1, t_2) \stackrel{\text{def}}{=} \frac{1}{2}\mathrm{E}[\tilde{Y}_a(t_1)^*\tilde{Y}_b(t_2)] = \int \tilde{x}_a(t_1 - \tau)^* \tilde{x}_b(t_2 - \tau)\phi_h(\tau; t_1, t_2)\, d\tau \tag{15}$$

and this holds for all low-pass $\tilde{x}_a(t)$ and $\tilde{x}_b(t)$.

Likewise, the arguments used to derive the autocorrelation function spatial integral expression (14) in Appendix B are easily modified to consider two fictitious channels with identical scattering fields, but different input signals. The result is

$$R_{\tilde{Y}_a\tilde{Y}_b}(t_1, t_2) = \int_{\tau_0}^{\infty} \tilde{x}_a(t_1 - \tau)^* \tilde{x}_b(t_2 - \tau) \times \left\{ \int_{-\pi}^{\pi} \mathcal{L}_1(\tau, \theta)\mathcal{L}_2(\tau, \theta)\phi_S(\tau, \theta; \Delta t) \times J(\tau, \theta)e^{j2\pi\lambda(\tau, \theta)(t_2 - t_1)}\, d\theta \right\} d\tau. \tag{16}$$

The expression in brackets $\{\cdot\}$ depends on t_2 and t_1 only through the time difference $\Delta t = t_2 - t_1$, which indicates a WSS channel. Thus, relating (16) to (15), we immediately identify

$$\phi_h(\tau; \Delta t) = \int_{-\pi}^{\pi} \psi(\tau, \theta; \Delta t)e^{j2\pi\lambda(\tau, \theta)\Delta t}\, d\theta \tag{17}$$

where

$$\psi(\tau, \theta; \Delta t) \stackrel{\text{def}}{=} \mathcal{L}_1(\tau, \theta)\mathcal{L}_2(\tau, \theta)\phi_S(\tau, \theta; \Delta t)J(\tau, \theta). \tag{18}$$

Note that the only Δt dependency in definition (18) is due to the scattering field intensity $\phi_S(\tau, \theta; \Delta t)$. In practice, this time variation is due to slow apparent fading of discrete scatterers as discussed in Section II. The factors in (18) are real valued, except for $\phi_S(\tau,\theta;\Delta t)$, which is a conjugate symmetric function of Δt.

B. The Stationary Base Station—$\phi_h(\tau;\Delta t)$

We now consider the case of a mobile transmitter and a stationary receiver. The transmitter's velocity vector is written $\mathbf{v}_T = v(\cos(\theta_0),\sin(\theta_0))$, where $v \geq 0$ is the mobile's speed and θ_0 is the mobile's direction angle relative to the transmitter-receiver baseline. By reciprocity, the results hold equally for a mobile receiver and a stationary transmitter. (Just reorient the coordinate system about the receiver.)

First, consider the Doppler frequency variable. Since $\mathbf{e}_T = (\cos(\theta),\sin(\theta))$, we have $\mathbf{e}_T\cdot\mathbf{v}_T = v\cos(\theta-\theta_0)$. Together with $\mathbf{v}_R = \mathbf{0}$, this reduces the Doppler expression (8) to

$$\lambda(\tau,\theta) = \lambda(\theta) \stackrel{\text{def}}{=} \lambda_m\cos(\theta-\theta_0) \tag{19}$$

where $\lambda_m = \frac{v}{c}f_c$ is the maximal Doppler shift. The delay cross-power density integral (17) then becomes

$$\phi_h(\tau;\Delta t) = \int_{-\pi}^{\pi}\psi(\tau,\theta;\Delta t)e^{j2\pi\lambda_m\cos(\theta-\theta_0)\Delta t}\,d\theta.$$

$\psi(\tau,\theta;\Delta t)$ is periodic in θ, and hence, the domain of integration may be taken to be any interval of length 2π. Applying the change of variables $\theta\to\theta+\theta_0$ and then centering the domain of integration yields

$$\phi_h(\tau;\Delta t) = \int_{-\pi}^{\pi}\psi(\tau,\theta+\theta_0;\Delta t)e^{j2\pi\lambda_m\cos(\theta)\Delta t}\,d\theta. \tag{20}$$

Next, expand $\psi(\tau,\theta;\Delta t)$ into the Fourier series $\sum_{n=-\infty}^{\infty}\psi_n(\tau;\Delta t)e^{jn\theta}$. The series coefficients are

$$\psi_n(\tau;\Delta t) = \frac{1}{2\pi}\int_{-\pi}^{\pi}\psi(\tau,\theta;\Delta t)e^{-jn\theta}\,d\theta. \tag{21}$$

Applying the Fourier series to (20) yields

$$\phi_h(\tau;\Delta t) = \sum_{n=-\infty}^{\infty}\psi_n(\tau;\Delta t)e^{jn\theta_0}\int_{-\pi}^{\pi}e^{j[2\pi\lambda_m\cos(\theta)\Delta t+n\theta]}\,d\theta.$$

Using the Bessel functions identity $\int_{-\pi}^{\pi}e^{j[z\cos(\theta)+n\theta]}\,d\theta = 2\pi j^n J_n(z)$, the last series is reduced to

$$\phi_h(\tau;\Delta t) = 2\pi\sum_{n=-\infty}^{\infty}j^n\psi_n(\tau;\Delta t)e^{jn\theta_0}J_n(2\pi\lambda_m\Delta t). \tag{22}$$

The series (22) can be further reduced to a single-sided series for the case that $\phi_S(\tau,\theta;\Delta t)$ is a strictly real-valued function, and hence, so is $\psi(\tau,\theta;\Delta t)$. In this case, $\psi_n(\tau;\Delta t)$ has conjugate symmetry in n. Since $J_{-n}(z) = (-1)^n J_n(z)$, we get

$$\phi_h(\tau;\Delta t) = 2\pi\Bigg\{\psi_0(\tau;\Delta t)J_0(2\pi\lambda_m\Delta t) + 2\sum_{n=1}^{\infty}j^n\,\mathrm{Re}\big\{\psi_n(\tau;\Delta t)e^{jn\theta_0}\big\}J_n(2\pi\lambda_m\Delta t)\Bigg\}. \tag{23}$$

C. The Stationary Base Station—$S_h(\tau;\lambda)$

A series for the scattering function is obtained from the Fourier transform relationship

$$\int J_n(2\pi\lambda_m\Delta t)e^{-j2\pi\lambda\Delta t}\,d\Delta t = \frac{F_n(\lambda/\lambda_m)}{j^n 2\pi\lambda_m}$$

where

$$F_n(z) \stackrel{\text{def}}{=} 2\frac{\cos(\,n\cos^{-1}(z)\,)}{\sqrt{1-z^2}} \tag{24}$$

for $|z|\leq 1$, and $F_n(z) = 0$ for $|z| > 1$. Also, define the coefficient transforms

$$\Psi_n(\tau;\lambda) \stackrel{\text{def}}{=} \int_{-\infty}^{\infty}\psi_n(\tau;\Delta t)e^{-j2\pi\lambda\Delta t}\,d\Delta t. \tag{25}$$

Then, Fourier transform of (22) is

$$S_h(\tau;\lambda) = \frac{1}{\lambda_m}\sum_{n=-\infty}^{\infty}e^{jn\theta_0}\Psi_n(\tau;\lambda) * F_n\left(\frac{\lambda}{\lambda_m}\right).$$

where the convolution is with respect to the Doppler variable λ. Combining (25) and (21), we find that $\Psi_n(\tau;\lambda)$ can also be expressed as

$$\Psi_n(\tau;\lambda) = \frac{1}{2\pi}\int_{-\pi}^{\pi}\Psi(\tau,\theta;\lambda)e^{-jn\theta}\,d\theta$$

where $\Psi(\tau,\theta;\lambda) \stackrel{\text{def}}{=} \int\psi(\tau,\theta;\Delta t)\,e^{-j2\pi\lambda\Delta t}\,d\Delta t$. Since $\psi(\tau,\theta;\Delta t)$ is a conjugate symmetric nonnegative definite function of Δt, it follows that $\Psi(\tau,\theta;\lambda)$ is real valued and nonnegative, which in turn implies that $\Psi_n(\tau;\lambda)$ has conjugate symmetry in n. This conjugate symmetry is used to reduce the last scattering function series to

$$S_h(\tau;\lambda) = \frac{1}{\lambda_m}\Bigg\{\Psi_0(\tau;\lambda) * F_0(\lambda) + 2\sum_{n=1}^{\infty}\mathrm{Re}\big\{\Psi_n(\tau;\lambda)e^{jn\theta_0}\big\} * F_n\left(\frac{\lambda}{\lambda_m}\right)\Bigg\}. \tag{26}$$

The resulting series is clearly real valued, as it must be. For very slow fading scattering fields, we very nearly have $\Psi_n(\tau;\lambda) \approx \psi_n(\tau)\delta(\lambda)$. This leads to obvious reduction of (26).

We can also derive a direct expression for $S_h(\tau;\lambda)$ for the case of a time-invariant scattering field (that is, $\phi_S(\mathbf{r};\Delta t) \equiv \phi_S(\mathbf{r})$). The first step is to apply the transformation $\theta \to \lambda = \lambda_m\cos(\theta)$ to (20). This transformation is not one-to-one; we must split the θ integral into two parts. For $\theta \in [-\pi,0)$, we have $\theta = -\cos^{-1}(\lambda/\lambda_m)$ and $\sin(\theta) = \sqrt{1-\cos(\theta)^2} = \sqrt{1-(\lambda/\lambda_m)^2}$. This implies $d\lambda = \lambda_m\sin(\theta)\,d\theta = \sqrt{\lambda_m^2-\lambda^2}\,d\theta$ or $d\theta = d\lambda/\sqrt{\lambda_m^2-\lambda^2}$. For $\theta \in [0,\pi)$, we have $\theta = \cos^{-1}(\lambda/\lambda_m)$ and $d\theta = -d\lambda/\sqrt{\lambda_m^2-\lambda^2}$, but the negative sign in the $d\lambda$ differential will be used to flip the limits of integration. Combining the two resulting $d\lambda$ integrals, (20) becomes the equation given at

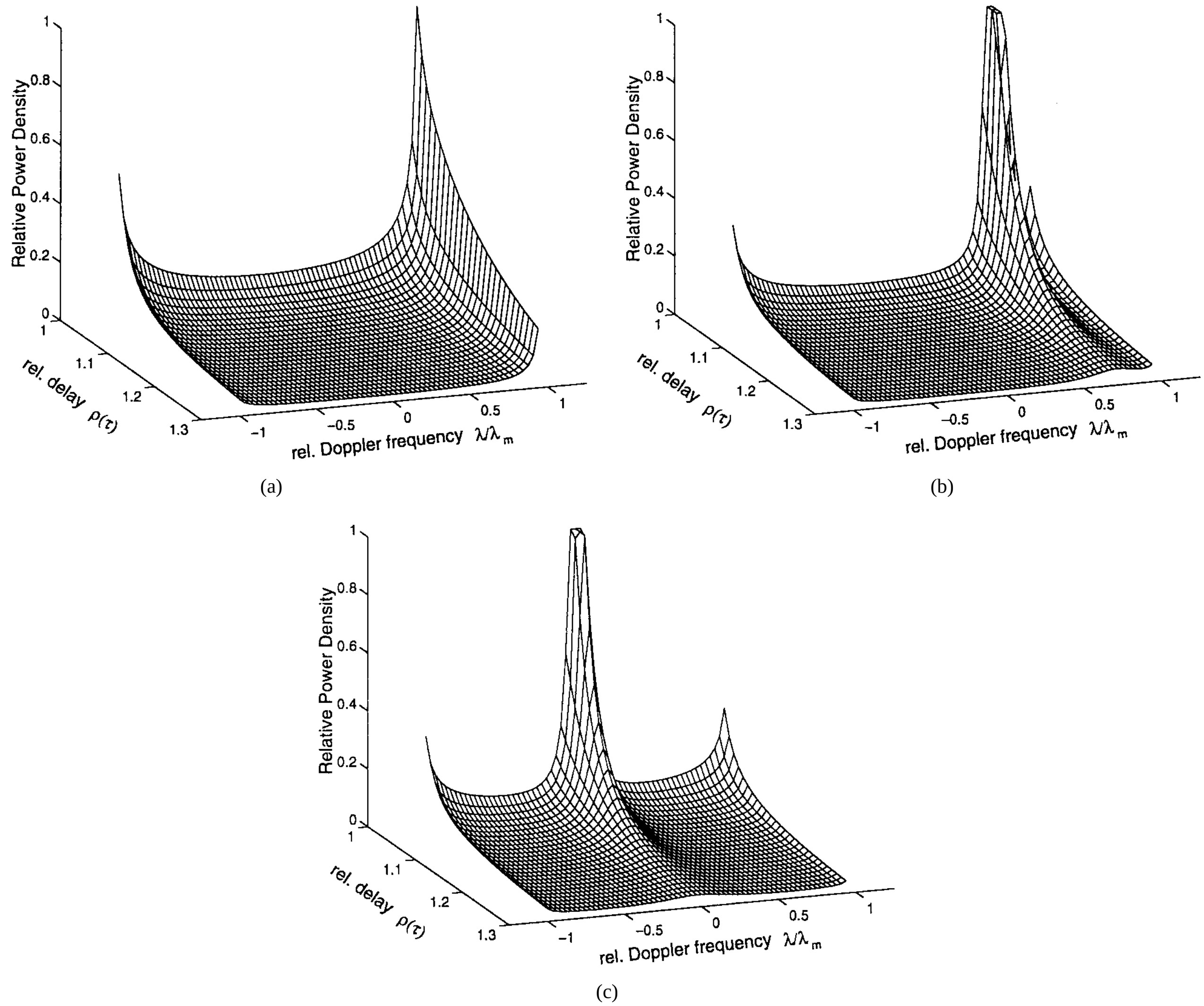

Fig. 2. Rural/suburban model scattering function for (a) $\theta_0 = 0°$, (b) $\theta_0 = 45°$, and (c) $\theta_0 = 90°$.

the bottom of the page. This last integral is an inverse Fourier transform. Thus, we deduce

$$S_h(\tau;\lambda) = \frac{\psi(\tau, \theta_0 - \cos^{-1}(\lambda/\lambda_m)) + \psi(\tau, \theta_0 + \cos^{-1}(\lambda/\lambda_m))}{\sqrt{\lambda_m^2 - \lambda^2}}. \quad (27)$$

D. Delay/Temporal Separability

$J_0(0) = 1$ and $J_n(0) = 0$ for $n \neq 0$, and, hence, from (22), we find that multipath intensity profile is

$$\phi_h(\tau) \stackrel{\text{def}}{=} \phi_h(\tau; 0) = 2\pi\psi_0(\tau; 0). \quad (28)$$

This function depends only on the spatial statistics of the scattering field and loss model and not on the mobile velocity $\mathbf{v}$. Moreover, observe that the zeroth term of (22) clearly corresponds to the classical result. This term depends on $\mathbf{v}_T$ only through the speed v (via $\lambda_m = \frac{v}{c} f_c$) and not the mobile's direction θ_0. In fact, since $\int_{-\pi}^{\pi} \psi_n(\tau) e^{jn\theta_0}\, d\theta_0 = 0$ for $n \neq 0$, averaging with respect to mobile direction θ_0 reduces the series (22) to the satisfying result

$$\frac{1}{2\pi}\int_{-\pi}^{\pi} \phi_h(\tau; \Delta t)\, d\theta_0 = 2\pi\psi_0(\tau; \Delta t) J_0(2\pi\lambda_m \Delta t) \approx \phi_h(\tau) J_0(2\pi\lambda_m\Delta t) \quad (29)$$

where the approximation holds for very slow fading or time-invariant scattering fields. Of course, this last result is the delay/temporal separability discussed in the introduction.

IV. Examples

In this section, we present some numerical examples. We consider only time-invariant and uniformly distributed spatial

$$\phi_h(\tau; \Delta t) = \int_{-\lambda_m}^{\lambda_m} \frac{\psi(\tau, \theta_0 - \cos^{-1}(\lambda/\lambda_m)) + \psi(\tau, \theta_0 + \cos^{-1}(\lambda/\lambda_m))}{\sqrt{\lambda_m^2 - \lambda^2}} e^{j2\pi\lambda\Delta t}\, d\lambda.$$

scattering fields, that is, $\phi_S(\mathbf{r};\Delta t) \equiv \phi_S =$ constant. In the first example, the loss factors are $\mathcal{L}_i(\mathbf{r}) = C_L/r_i^2$. As discussed in the introduction, this type of model would be appropriate for a sparse scattering field, as in the rural or suburban case. Strong shadowing effects must be accounted for in the urban environment. We thus present two examples with $\mathcal{L}_1(\mathbf{r}) = C_L e^{-r_1/\bar{r}}/r_1^2$. The factor $e^{-r_1/\bar{r}}$ represents the mean-square value of the $\mathbf{r}_T \to \mathbf{r}$ shadowing (which could be a lognormal random variable). The two examples of this type are $\bar{r} = r_0$ and $\bar{r} = 0.2r_0$, which represent, respectively, the situation when the mobile is near the base station and on the cell boundary.

A. The Rural/Suburban Model

For the case $\mathcal{L}_i(\mathbf{r}) = C_L/r_i^2$, we can determine some explicit closed from expressions for the Bessel series coefficients. First, plug the Jacobian expression (36) from Appendix A into (18) (and use (35) to eliminate r_2). This yields

$$\psi(\tau,\theta) = C\frac{1}{\rho(\tau)^2-1}\frac{\rho(\tau)-\cos(\theta)}{\rho(\tau)^2-2\cos(\theta)\rho(\tau)+1} \tag{30}$$

where $C = 4cC_L^2\phi_S/r_0^3$ and $\rho(\tau) \overset{\text{def}}{=} \tau/\tau_0$. By partial fractions expansion we obtain

$$\frac{\rho-\cos(\theta)}{\rho^2-2\cos(\theta)\rho+1} = \frac{1}{2}\left\{\frac{1}{\rho-e^{j\theta}}+\frac{1}{\rho-e^{-j\theta}}\right\}.$$

Applying the above identity to the previous display and then expanding the geometric series, we obtain

$$\begin{aligned}\psi(\tau,\theta) &= \frac{C/2}{\rho(\tau)(\rho(\tau)^2-1)}\left\{\frac{1}{1-\rho(\tau)^{-1}e^{j\theta}}+\frac{1}{1-\rho(\tau)^{-1}e^{-j\theta}}\right\}\\ &= \frac{C/2}{\rho(\tau)(\rho(\tau)^2-1)}\left\{\sum_{n=0}^{\infty}\rho(\tau)^{-n}e^{jn\theta}+\sum_{n=0}^{\infty}\rho(\tau)^{-n}e^{-jn\theta}\right\}\\ &= \frac{C/2}{\rho(\tau)(\rho(\tau)^2-1)}\left\{1+\sum_{n=-\infty}^{\infty}\rho(\tau)^{-|n|}e^{jn\theta}\right\}.\end{aligned}$$

From this, we deduce that

$$\psi_0(\tau) = \frac{C}{\rho(\tau)(\rho(\tau)^2-1)} \tag{31}$$

and

$$\psi_n(\tau) = \frac{1}{2}\psi_0(\tau)\rho(\tau)^{-|n|} \tag{32}$$

for $n \neq 0$.

As the delay is reduced to the minimal delay τ_0, equivalently, as $\rho(\tau) \downarrow 1$, the coefficients $\psi_n(\tau) \uparrow \infty$. This singularity is a result of the $\propto 1/r^2$ loss model. Of course, $\mathcal{L}(r) \propto 1/r^2$ is not physically justifiable within the antenna's near field. Thus, (32) is valid only when the distance $c\tau - r_0$ is larger than the near field radius.

Finally, applying (30) and (31) to (27) yields the closed-form expression

$$\begin{aligned}S_h(\tau;\lambda) = \frac{\psi_0(\tau)}{\sqrt{\lambda_m^2-\lambda^2}} &\times\left\{\frac{\rho(\tau)[\rho(\tau)-\cos(\theta_0+\cos^{-1}(\lambda/\lambda_m))]}{\rho(\tau)^2-2\rho(\tau)\cos(\theta_0+\cos^{-1}(\lambda/\lambda_m))+1}\right.\\ &\left.+\frac{\rho(\tau)[\rho(\tau)-\cos(\theta_0-\cos^{-1}(\lambda/\lambda_m))]}{\rho(\tau)^2-2\rho(\tau)\cos(\theta_0-\cos^{-1}(\lambda/\lambda_m))+1}\right\}.\end{aligned} \tag{33}$$

Fig. 2 illustrates several scattering functions computed using (33). The cases are $\theta_0 = 0°$, $\theta_0 = 45°$, and $\theta_0 = 90°$. For directions of travel $\theta_0 > 90°$, simply flip the λ axis for the $90° - \theta_0$ scattering function. The impact of the direction of travel is clearly apparent. As θ_0 ranges from 0° when the mobile is traveling directly toward the base to 180° when the mobile is traveling directly away from the base, the dominant Doppler shifts from $+\lambda_m$ to $-\lambda_m$.

B. The Urban Model

As an example of an urban model, we modify the above model to have scatterer-to-mobile mean-square loss $\mathcal{L}_1(\mathbf{r}) = C_L e^{-r_1/\bar{r}}/r_1^2$. It is presumed that the base station is in a prominent position so that shadowing is not a significant factor on the base-to-scatterer path. Thus, we retain $\mathcal{L}_2(\mathbf{r}) = C_L/r_2^2$.

It is not possible to obtain closed-form expressions for Bessel series coefficients for the urban model. Likewise, the closed-form expression for the scattering function (27) cannot be reduced to a compact expression, as we have done for the rural/suburban model in (33). Nonetheless, the loss model and Jacobian formulas (from Appendix A) can be used to evaluate $\psi(\tau,\theta_0 \pm \cos^{-1}(\lambda/\lambda_m))$ point-by-point. Thus, (27) is easily evaluated numerically. Figs. 3 and 4 illustrate these numerically computed scattering functions again for $\theta_0 = 0°$, $\theta_0 = 45°$, and $\theta_0 = 90°$. Fig. 3 shows the case $\bar{r} = r_0$, which would be typical of the case when the mobile is near the base. Fig. 4 shows the case $\bar{r} = 0.2r_0$, which might be typical of the case when the mobile is far from the base, hence, near the cell boundary.

C. Ensemble Averaging

It should be understood that the statistical expectations used to define the delay cross-power density and the scattering function are *ensemble averages*. An empirically measured scattering function, or one generated by simulation, may differ significantly from the ensemble average result. This is particularly true for scattering fields characterized by a sparse distribution of discrete scatterers.

Fig. 5 illustrates this point. Fig. 5(a) and (b) shows two "snap-shot" simulations of the rural/suburban model with $\theta_0 = 45°$. Roughly 20 discrete scatterers are distributed on the plane according to a spatial Poisson distribution. Each scatterer results in a single line in the scattering function. These simulations do not include the apparent slow fading due to compound scatterers, as discussed in Section II-D. Fig. 5(c) shows the result of averaging 10 000 snap-shot simulations of the type illustrated in 5(a) and (b). Fig. 5(c) is very similar to the ensemble average result plotted in Fig. 2(b).

V. Conclusion

We have presented a new analysis of the mobile WSSUS channel model without imposing the assumption of uniformly distributed angles of arrival. Our results are determined by the

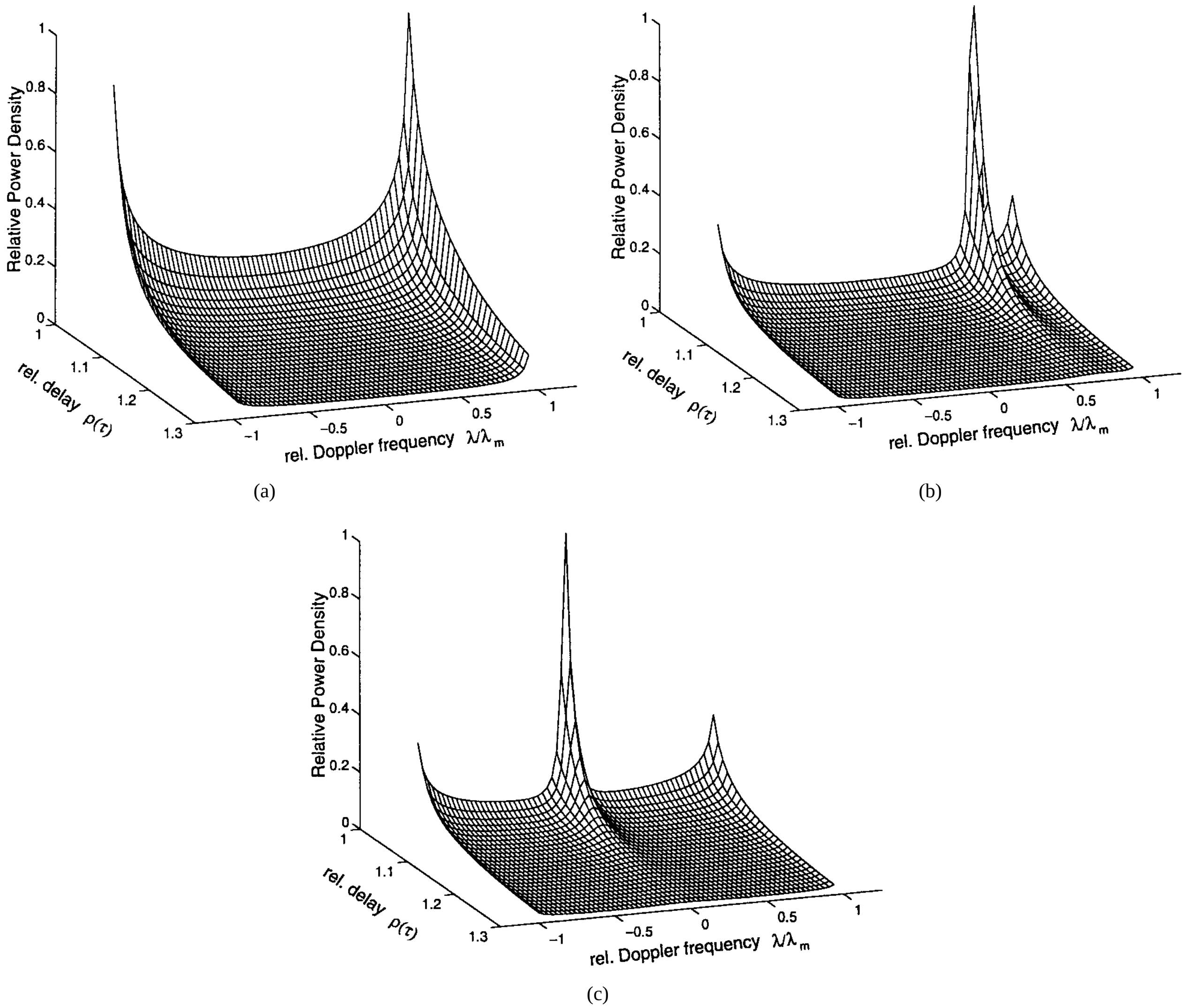

Fig. 3. Urban model scattering function with $\bar{r}_1 = r_0$ for (a) $\theta_0 = 0°$, (b) $\theta_0 = 45°$, and (c) $\theta_0 = 90°$.

spatial scattering intensity function and the propagation-loss model. We have worked through to give precise expressions for the Bessel series coefficients only for the case of a uniform scattering field.

We obtain our best results for the case of a time-invariant scattering field, that is, $Z(\mathbf{r};t) \equiv Z(\mathbf{r})$. For this case, we obtained the closed-form expression for the scattering function (27), and in Section IV, we presented several numerical examples that utilize this expression. As discussed in Section II, a physical scatterer (having dimensions smaller that the spatial resolution $c/2W$) can be modeled as a slow fading point scatterer. In this case, the delay cross-power density and scattering function can be numerically evaluated using the Bessel series results of Section III-B and C. For fixed τ and Δt, evaluate $\psi(\tau, 2\pi m/M; \Delta t)$ for $m = 0, \cdots, M-1$ and then apply the FFT to get the series coefficients.

Appendix A
The Transformation $\mathbf{r} \to (\tau, \theta)$

In this Appendix, we consider the transformation $\mathbf{r} \to (\tau, \theta)$ with $\mathbf{r}_T = \mathbf{0}$ and $\mathbf{r}_R = (r_0, 0)$. We write $\mathbf{r} = (x, y)$, $r_1 = \|\mathbf{r}\| = \sqrt{x^2 + y^2}$ and $r_2 = \|\mathbf{r} - \mathbf{r}_R\| = \sqrt{(x - r_0)^2 + y^2}$.

First, we derive expressions of r_1 and r_2 as functions of (τ, θ). The law of cosines gives $r_0^2 + r_1^2 - 2r_0 r_1 \cos(\theta) = r_2^2$. Since $c\tau = r_1 + r_2$, we may equate the law of cosines to $r_2^2 = (c\tau - r_1)^2$. Define $\rho = \rho(\tau) \stackrel{\text{def}}{=} c\tau/r_0$. Solving for r_1 yields

$$r_1(\tau, \theta) = \frac{\rho^2 - 1}{2(\rho - \cos(\theta))} r_0 \tag{34}$$

and from $r_2 = c\tau - r_1$

$$r_2(\tau, \theta) = \frac{\rho^2 - 2\rho\cos(\theta) + 1}{2(\rho - \cos(\theta))} r_0. \tag{35}$$

Next, we derive the Jacobian formula. Since $\tau = (r_1 + r_2)/c$, we have

$$\frac{\partial \tau}{\partial x} = \frac{1}{c}\left\{\frac{x}{r_1} + \frac{x - r_0}{r_2}\right\} \quad \text{and} \quad \frac{\partial \tau}{\partial y} = \frac{1}{c}\left\{\frac{y}{r_1} + \frac{y}{r_2}\right\}.$$

Using $\sin(\theta) = y/r_1$, $\cos(\theta) = x/r_1$, $\partial r_1^{-1}/\partial x = -x/r_1^3$ and $\partial r_1^{-1}/\partial y = -y/r_1^3$, we have

$$\cos(\theta)\frac{\partial \theta}{\partial x} = y\frac{-x}{r_1^3} \Rightarrow \frac{\partial \theta}{\partial x} = \frac{-y}{r_1^2}$$

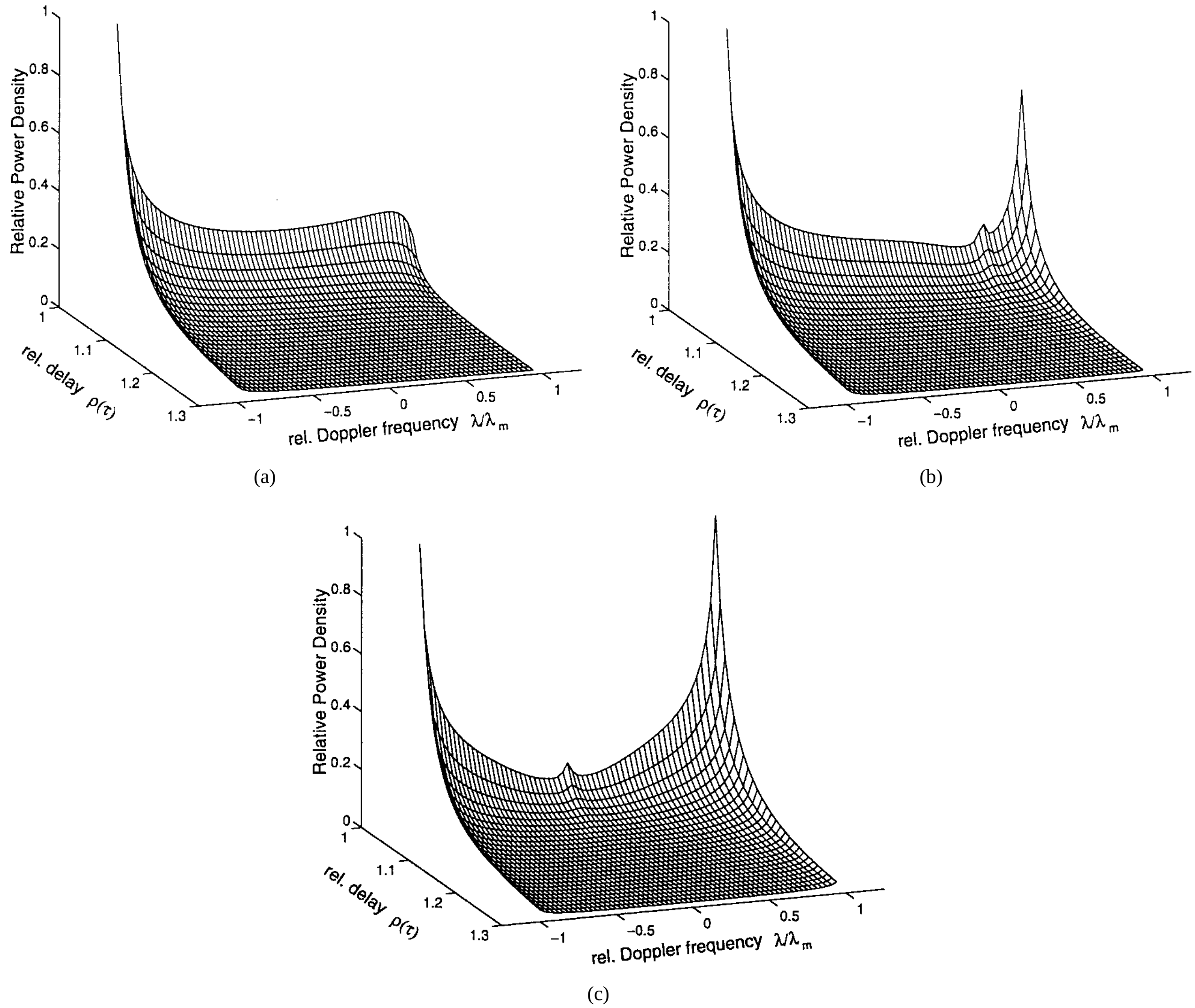

Fig. 4. Urban model scattering function with $\bar{r}_1 = 0.2r_0$ for (a) $\theta_0 = 0°$, (b) $\theta_0 = 45°$, and (c) $\theta_0 = 90°$.

and

$$-\sin(\theta)\frac{\partial\theta}{\partial y} = x\frac{-y}{r_1^3} \Rightarrow \frac{\partial\theta}{\partial y} = \frac{-x}{r_1^2}.$$

The above results are now used to evaluate

$$D = \det\begin{bmatrix} \frac{\partial\tau}{\partial x} & \frac{\partial\tau}{\partial y} \\ \frac{\partial\theta}{\partial x} & \frac{\partial\theta}{\partial y} \end{bmatrix} = \frac{r_1 r_2 + r_1^2 - r_0 x}{c r_1^2 r_2}.$$

The law of cosines $r_0^2 + r_1^2 - 2r_0 r_1 \cos(\theta) = r_2^2$ yields $r_0 x = r_0 r_1 \cos(\theta) = (r_0^2 + r_1^2 - r_2^2)/2$, and, hence,

$$D = \frac{2r_1 r_2 + 2\,r_1^2 - \left(r_0^2 + r_1^2 - r_2^2\right)}{2cr_1^2 r_2} = \frac{(r_1 + r_2)^2 - r_0^2}{2cr_1^2 r_2}.$$

Using $c\tau = r_1 + r_2 > r_0$, we have

$$J(\tau, \theta) = \frac{1}{|D|} = \frac{2c\,r_1^2 r_2}{(c\tau)^2 - r_0^2}. \tag{36}$$

Finally, apply (34) and (35) to eliminate r_1 and r_2. The result is

$$J(\tau, \theta) = \frac{cr_0}{4}\frac{(\rho^2 - 1)(\rho^2 - 2\cos(\theta)\rho + 1)}{(\rho - \cos(\theta))^3}. \tag{37}$$

Appendix B
Proper Complex Symmetry

This Appendix derives the results stated in Section II-E. Recall that we assume conditions 1)–3) as stated in Section II-E.

Utilizing the independence condition 1), the expectation of formula (11) is

$$\mathrm{E}[\tilde{Y}(t)] = \int \tilde{x}(t - \tau(\mathbf{r}))\mathrm{E}[L(\mathbf{r}; t)]\mu_S(\mathbf{r}) \times e^{-j2\pi[f_c\tau(\mathbf{r}) - \lambda(\mathbf{r})(t-t_1)]}\,d\mathbf{r}.$$

Applying the transformation $\mathbf{r} \rightarrow (\tau, \theta)$ yields

$$\mathrm{E}[\tilde{Y}(t)] = \int_{-\pi}^{\pi}\int_{\tau_0}^{\infty} \tilde{x}(t - \tau)\mathrm{E}[L(\tau, \theta; t)]\mu_S(\tau, \theta; t)J(\tau, \theta) \times e^{j2\pi\lambda(\tau,\theta)(t-t_1)}e^{-j2\pi f_c\tau}\,d\tau\,d\theta.$$

Now consider $\tilde{x}(t - \tau)\mathrm{E}[L(\tau, \theta; t)]\mu_S(\tau, \theta; t)$ as a function of τ. By conditions 2) and 3), the bandwidth of this function is essentially the bandwidth of $\tilde{x}(t - \tau)$, that is, $W \ll f_c$. The Jacobian $J(\tau, \theta)$ and the Doppler frequency $\lambda(\tau, \theta)$ will

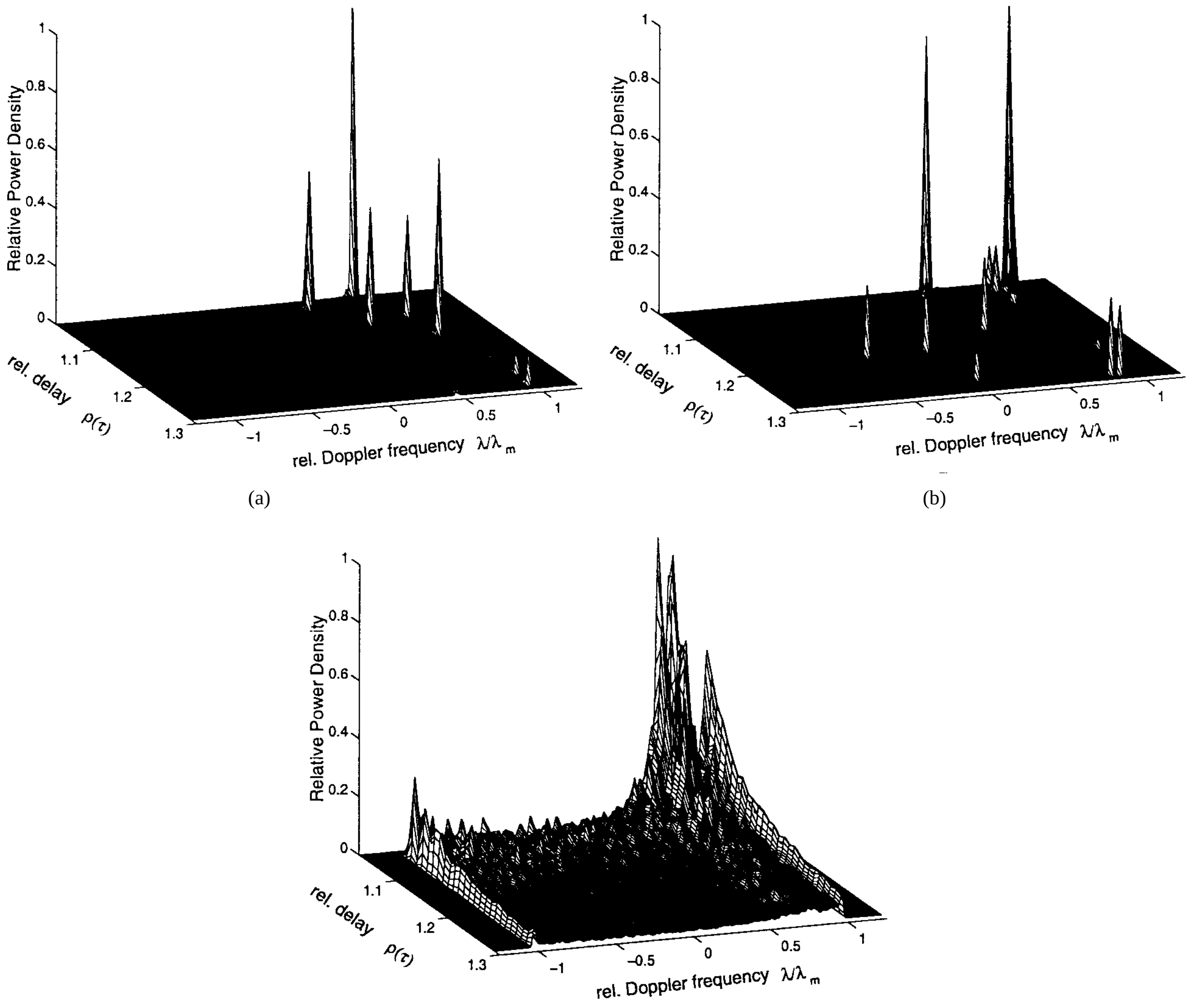

(a) (b) (c)

Fig. 5. Snap shots [(a) and (b)] versus an ensemble average and (c) $\theta_0 = 45°$, rural/suburban model.

likewise be very slowly varying functions of τ. [In fact, for the case of a stationary base, $\lambda(\tau,\theta) = \lambda(\theta)$ does not depend on τ at all]. Thus, integrand of the $d\tau$ integral is a low-pass function of τ modulated by $e^{-j2\pi f_c \tau}$. The narrowband approximation thus yields $\mathrm{E}[\tilde{Y}(t)] \approx 0$.

There is a weakness in the above argument. The Jacobian $J(\tau,\theta)$ is singular on the baseline between the transmitter and receiver, and hence, $J(\tau,\theta)$ is not a slowly varying function of τ near the minimal delay $\tau_0 = r_0/c$. The question that we must address is how close to τ_0 is the approximation valid? We address this issue using the condition that the relative change of $J(\tau,\theta)$ over one carrier wave period $1/f_c$ should be small. Formally, we consider the condition

$$\frac{|\partial J(\tau,\theta)/\partial\tau|(1/f_c)}{J(\tau,\theta)} \ll 1.$$

Put $\delta = \rho - 1$ and write $J(\tau,\theta) = (cr_0/4)\frac{a}{b^3}$, where after some algebra $a(\delta) = \delta(\delta+2)(\delta^2 + 4(\delta+1)\sin(\theta/2)^2)$ and $b(\delta) = \delta + 2\sin(\theta/2)^2$. Then, using $\partial\delta/\partial\tau \equiv c/r_0$ and $\partial b/\partial\delta \equiv 1$, we get

$$\frac{\partial J/\partial\tau}{J} = \frac{c}{r_0}\frac{b^3}{a}\left\{\frac{\partial a/\partial\delta}{b^3} - \frac{3a}{b^4}\right\} = \frac{c}{r_0}\left\{\frac{\partial a/\partial\delta}{a} - \frac{3}{b}\right\}.$$

Substituting in expressions for $a(\delta)$, $\partial a/\partial\delta$ and $b(\delta)$ yields

$$\frac{\partial J/\partial\tau}{J} = \frac{c}{r_0}\left\{\frac{4\delta^3 + 6\delta^2 + 4(3\delta^2 + 6\delta + 2)\sin(\theta/2)^2}{\delta(\delta+2)(\delta^2 + 4(\delta+1)\sin(\theta/2)^2)} - \frac{3}{\delta + 2\sin(\theta/2)^2}\right\}. \quad (38)$$

Clearly we see that (38) is singular as $\delta \downarrow 0$ (equivalently, as $\rho \downarrow 1$). The approach here is to determine the small δ behavior of (38). Ultimately, we want to determine the smallest values of δ for which $|(\partial J/\partial\tau)/J| \ll f_c$. First, we must examine the role of the variable θ. As $|\theta|$ ranges from zero to π, $2\sin(\theta/2)^2$ is a strictly increasing function of $|\theta|$, and hence, the worst case values of θ are those near zero. Consider the spatial integral only on the half plane $x \leq r_0/2$. This determines a minimal value $|\theta|$, denoted $\theta_{\min}$, as illustrated in Fig. 6. In Fig. 6, $r_1 = c\tau/2 = \frac{r_0}{2}(1+\delta)$, and, hence,

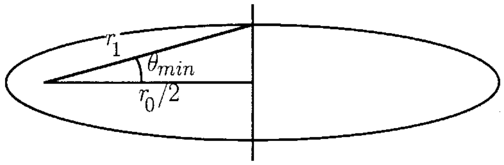

Fig. 6. Determination of $\theta_{\min}$.

$\theta_{\min} = \cos^{-1}(1/(1+\delta))$. For small δ, which implies small $\theta_{\min}$, we have $\cos(\theta_{\min}) = 1/(1+\delta) \sim 1-\delta$ and $\cos(\theta_{\min}) \sim 1-\theta_{\min}^2/2$, which implies $2\sin(\theta_{\min}/2)^2 \sim \theta_{\min}^2/2 \sim \delta$. Thus, when collecting the dominant small δ terms, we must take care not to eliminate the appropriate $2\sin(\theta/2)^2$ terms.

Now, eliminate the small δ negligible terms in (38), for example, $\delta+2 \sim 2$ and $\delta^2+\delta \sim \delta$. We treat the $2\sin(\theta/2)^2$ terms as $\sim\delta$ to handle values $|\theta|$ near $\theta_{\min}$. The result is

$$\frac{\partial J/\partial\tau}{J} \sim \frac{c}{r_0}\left\{\frac{1}{\delta} - \frac{3}{\delta+2\sin(\theta/2)^2}\right\}. \tag{39}$$

For $|\theta| \gg \theta_{\min}$, the second term is negligible, and we have $(\partial J/\partial\tau)/J \sim c/(r_0\delta)$. For $|\theta|$ near $\theta_{\min}$, using $2\sin(\theta/2)^2 \sim \delta$, we obtain $(\partial J/\partial\tau)/J \sim -c/(2r_0\delta)$. We thus conclude that the condition $|(\partial J/\partial\tau)/J| \ll f_c$ is equivalent to $c/(2r_0\delta) \ll f_c$ or equivalently

$$\tau - \tau_0 = \frac{r_0\delta}{c} \gg \frac{1}{2f_c}$$

which is the condition stated in Section II-E. The above arguments hold only for spatial integrals over the half plane $x \le r_0/2$. For the other half plane, we simply reorient the coordinate system about the receiver in Fig. 1 rather than the transmitter. By the obvious symmetry, the results are the same.

Now, consider the pseudo autocorrelation. Again, starting with (11), we obtain

$$\begin{aligned}
&\mathrm{E}[\tilde{Y}(t_1)\tilde{Y}(t_2)] \\
&\quad = \iint \tilde{x}(t_1-\tau(\mathbf{r}))\tilde{x}(t_2-\tau(\mathbf{r}'))\mathrm{E}[L(\mathbf{r};t_1)L(\mathbf{r}';t_2)] \\
&\qquad \times \mathrm{E}[Z(\mathbf{r};t_1)Z(\mathbf{r}';t_2)]e^{j2\pi\lambda(\mathbf{r}')\Delta t} \\
&\qquad \times e^{-j2\pi f_c[\tau(\mathbf{r})+\tau(\mathbf{r}')]}\,d\mathbf{r}\,d\mathbf{r}'.
\end{aligned}$$

The above display is expanded into two integrals using the spatial US condition (4): $\mathrm{E}[Z(\mathbf{r};t_1)Z(\mathbf{r}';t_2)] = 2\hat{\phi}_S(\mathbf{r};\Delta t)\delta(\mathbf{r}'-\mathbf{r}) + \mu_S(\mathbf{r})\mu_S(\mathbf{r}')$. After applying the change of variables $\mathbf{r} \to (\tau,\theta)$, the integral resulting from $2\hat{\phi}_S(\mathbf{r};\Delta t)\delta(\mathbf{r}'-\mathbf{r})$ is

$$\begin{aligned}
&\int_{-\pi}^{\pi}\int_{\tau_0}^{\infty} \tilde{x}(t_1-\tau)\tilde{x}(t_2-\tau)\mathrm{E}[L(\tau,\theta;t_1)L(\tau,\theta;t_2)] \\
&\quad \times \hat{\phi}_S(\tau,\theta;\Delta t)J(\tau,\theta)e^{j2\pi\lambda(\tau,\theta)\Delta t}e^{-j2\pi(2f_c)\tau}\,d\tau\,d\theta.
\end{aligned}$$

By the same arguments as above, as a function of τ the bandwidth of the integrand of the $d\tau$ integral is essentially the bandwidth of $\tilde{x}(t_1-\tau)\tilde{x}(t_2-\tau)$, which is $2W$. But then the modulating frequency is $2f_c$. Thus, the above integral vanishes. Next, consider the integral resulting from $\mu_S(\mathbf{r})\mu_S(\mathbf{r}')$

$$\begin{aligned}
&\int_{-\pi}^{\pi}\int_{r_0/c}^{\infty}\left\{\int_{-\pi}^{\pi}\int_{\tau_0}^{\infty} z_1(\tau,\theta)\mathrm{E}[L(\tau,\theta;t_1)L(\tau',\theta';t_2)]\right. \\
&\qquad \left.\times\, e^{-j2\pi f_c\tau}\,d\tau\,d\theta\right\} z_2(\tau',\theta')e^{j2\pi\lambda(\tau',\theta')\Delta t} \\
&\qquad \times e^{-j2\pi f_c\tau'}\,d\tau'\,d\theta'.
\end{aligned}$$

where we write $z_i(\tau,\theta) = \tilde{x}(t_i-\tau)\mu_S(\tau,\theta)J(\tau,\theta)$ to minimize the notation. For fixed (τ',θ'), the integral in brackets $\{\cdot\}$ is again seen to be the integral of a modulated low-pass function, so it too vanishes.

We have now shown that the mean and pseudo-autocorrelation function of the channel response $\tilde{Y}(t)$ vanish: $\mathrm{E}[\tilde{Y}(t)] \approx 0$ and $\mathrm{E}[\tilde{Y}(t_1)\tilde{Y}(t_2)] \approx 0$. Thus, $\tilde{Y}(t)$ has proper complex symmetry.

Finally, the complex autocorrelation function is similarly obtained from (11). We have

$$\begin{aligned}
&\mathrm{E}[\tilde{Y}(t_1)^*\tilde{Y}(t_2)] \\
&\quad = \iint \tilde{x}(t_1-\tau(\mathbf{r}))^*\tilde{x}(t_2-\tau(\mathbf{r}'))\mathrm{E}[L(\mathbf{r};t_1)^*L(\mathbf{r}';t_2)] \\
&\qquad \times \mathrm{E}[Z(\mathbf{r};t_1)^*Z(\mathbf{r}';t_2)]e^{j2\pi\lambda(\mathbf{r}')\Delta t} \\
&\qquad \times e^{j2\pi f_c(\tau(\mathbf{r})-\tau(\mathbf{r}'))}\,d\mathbf{r}\,d\mathbf{r}'.
\end{aligned}$$

By (3), we have $\mathrm{E}[Z(\mathbf{r};t_1)^*Z(\mathbf{r}';t_2)] = 2\phi_S(\mathbf{r};\Delta t)\delta(\mathbf{r}'-\mathbf{r}) + \mu_S(\mathbf{r})^*\mu_S(\mathbf{r}')$. With very minor changes, the same argument as in the previous paragraph is used to deduce that the $\mu_S(\mathbf{r})^*\mu_S(\mathbf{r}')$ integral vanishes. In condition 2), we assume that the moments of the losses $L_i(\mathbf{r};t)$ are essentially constant functions of t. Recalling $L(\mathbf{r};t) = L_1(\mathbf{r};t)L_2(\mathbf{r};t)$ by condition 2), we have $\mathrm{E}[L(\mathbf{r};t_1)^*L(\mathbf{r}';t_2)] = \mathcal{L}_1(\tau,\theta)\mathcal{L}_2(\tau,\theta)$, where we recall $\mathcal{L}_i(\mathbf{r}) \stackrel{\mathrm{def}}{=} \mathrm{E}[|L_i(\mathbf{r};t)|^2]$. Now, after applying the change of variables, the integral resulting from the term $\phi_S(\mathbf{r})\delta(\mathbf{r}'-\mathbf{r})$ yields

$$\begin{aligned}
R_{\tilde{Y}}(t_1,t_2) &= \int_{\tau_0}^{\infty}\tilde{x}(t_1-\tau)^*\tilde{x}(t_2-\tau) \\
&\quad \times \int_{-\pi}^{\pi}\mathcal{L}_1(\tau,\theta)\mathcal{L}_2(\tau,\theta)\phi_S(\tau,\theta;\Delta t)J(\tau,\theta) \\
&\quad \times e^{j2\pi\lambda(\mathbf{r})\Delta t}\,d\theta\,d\tau
\end{aligned}$$

which is precisely the desired expression (14).

References

[1] T. Aulin, "A modified model for the fading signal at a mobile radio channel," *IEEE Trans. Veh. Technol.*, vol. 28, pp. 182–203, Aug. 1979.

[2] A. S. Bajwa and J. D. Parsons, "Small-area characterization of UHF urban and suburban mobile radio propagation," *Proc. Inst. Elect. Eng.*, vol. 129, pt. F, pp. 102–109, 1982.

[3] P. A. Bello, "Characterization of randomly time-variant linear channels," *IEEE Trans. Commun.*, vol. 11, pp. 360–393, Dec. 1963.

[4] W. R. Braun and U. Dersch, "A physical mobile radio channel model," *IEEE Trans. Veh. Technol.*, vol. 40, pp. 472–482, May 1991.

[5] R. H. Clarke, "A statistical theory of mobile-radio reception," *Bell Syst. Tech. J.*, pp. 957–1000, July–Aug. 1968.

[6] D. C. Cox, "Delay Doppler characteristics of multipath propagation at 910 MHz in a suburban mobile radio environment," *IEEE Trans. Antennas Propagat.*, vol. 20, pp. 625–635, Sept. 1972.

[7] ——, "910 MHz urban mobile radio propagation: Multipath characteristics in New York City," *IEEE Trans. Commun.*, vol. 21, pp. 1188–1194, Nov. 1973.

[8] U. Dersch and R. J. Rüegg, "Simulations of the time and frequency selective outdoor mobile radio channel," *IEEE Trans. Veh. Technol.*, vol. 42, pp. 338–343, Aug. 1993.

[9] U. Dersch and E. Zollinger, "Propagation mechanisms in microcell and indoor environments," *IEEE Trans. Veh. Technol.*, vol. 43, pp. 1058–1066, Nov. 1994.

[10] B. Fleury and D. Dahlhaus, "Investigations on the time variations of the wide-band radio channel for random receiver movements," in *Proc. 3rd Int. Symp. Spread Spectrum Tech. Appl.*, Oulu, Finland, 1994, vol. 2, pp. 6.3.1–6.3.6.

[11] C. W. Helstrom, *Probability and Stochastic Processes for Engineers*, 2nd ed. New York: Macmillan, 1991.
[12] P. Hoeher, "A statistical discrete-time model for the WSSUS multipath channel," *IEEE Trans. Veh. Technol.*, vol. 41, pp. 461–468, Nov. 1992.
[13] W. C. Jakes, *Microwave Mobile Communications*. New York: Wiley, 1974.
[14] S. L. Lauritzen, C. Thommesen, and J. Bach Andersen, "A stochastic model in mobile communications," *Stochastic Process. Applicat.*, vol. 36, pp. 165–172, 1990.
[15] J. G. Proakis, *Digital Communications*, 3rd ed. New York: McGraw Hill, 1995.
[16] J. D. Parsons and A. S. Bajwa, "Wideband characterization of fading mobile radio channels," *Proc. Inst. Elect. Eng.*, vol. 129, pt. F, pp. 95–101, 1982.
[17] T. S. Rappaport, *Wireless Communications*. Upper Saddle River, NJ: Prentice-Hall, 1996.
[18] K.-W. Yip and T.-S. Ng, "Efficient simulation of digital transmission over WSSUS channels," *IEEE Trans. Commun.*, vol. 43, pp. 2907–2912, Dec. 1995.
[19] R. A. Ziegler and J. M. Cioffi, "Estimation of time-varying digital radio channels," *IEEE Trans. Veh. Technol.*, vol. 41, pp. 134–151, May 1992.

John S. Sadowsky (M'84) was born in Hammond, IN, in 1956. He received the B.S.E.E. and B.S.Ma. degrees from the Rose-Hulman Institute of Technology in 1978, the M.S.E.E. degree from Iowa State University, Ames, in 1981, and the M.A.Ma. and Ph.D. degrees in electrical engineering from the University of Wisconsin, Madison, respectively, in 1981 and 1984.

From 1978 to 1981, he was with Rockwell-Collins Avionics, Cedar Rapids, IA. His work at Collins included software development for aircraft energy management and area navigation and development of Kalman filters for GPS user equipment. From 1984 to 1993, he was with the faculty of the School of Electrical Engineering, Purdue University. In 1993, he joined the faculty of the Department of Electrical Engineering, Arizona State University, Tempe. Past and present research interests include applications of large deviations theory to problems in statistical communications theory, Monte Carlo simulation theory and application, and wireless communications systems.

Venceslav Kafedziski (S'94) received the Diploma and M.S. degrees in electrical engineering in 1982 and 1989, respectively, from the University Cyril and Methodius, Skopje, Macedonia. He is currently working toward the Ph.D. degree at Arizona State University, Tempe.

He was on the faculty of the University Cyril and Methodius from 1983 to 1990 and on leave from the same school at the Arizona State University from 1990 to 1991. His current research interests include digital communications and the applications of information and estimation theory and digital signal processing to wireless communications, with emphasis on joint-source channel coding, blind equalization, and the characterization, modeling, and capacity evaluation of time-varying channels.

Mr. Kafedziski was the recipient of a Graduate College Graduate Scholarship and supported by an NSF grant. He is a member of Phi Kappa Phi.